

Estimation of Surface and Top-of-Atmosphere Shortwave Irradiance in Biomass-Burning Regions during SCAR-B

SUNDAR A. CHRISTOPHER, XIANG LI, AND RONALD M. WELCH

Department of Atmospheric Sciences, University of Alabama in Huntsville, Huntsville, Alabama

JEFFREY S. REID

Atmospheric Propagation Branch-D858 Branch, Space and Naval Warfare System Center, San Diego, California

PETER V. HOBBS

Department of Atmospheric Sciences, University of Washington, Seattle, Washington

THOMAS F. ECK

Raytheon Corporation, and NASA Goddard Space Flight Center, Greenbelt, Maryland

BRENT HOLBEN

Biospheric Sciences Branch, NASA Goddard Space Flight Center, Greenbelt, Maryland

(Manuscript received 22 June 1999, in final form 14 December 1999)

ABSTRACT

Using in situ measurements of aerosol optical properties and ground-based measurements of aerosol optical thickness (τ_s) during the Smoke, Clouds and Radiation—Brazil (SCAR-B) experiment, a four-stream broadband radiative transfer model is used to estimate the downward shortwave irradiance (DSWI) and top-of-atmosphere (TOA) shortwave aerosol radiative forcing (SWARF) in cloud-free regions dominated by smoke from biomass burning in Brazil. The calculated DSWI values are compared with broadband pyranometer measurements made at the surface. The results show that, for two days when near-coincident measurements of single-scattering albedo ω_0 and τ_s are available, the root-mean-square errors between the measured and calculated DSWI for daytime data are within 30 W m^{-2} . For five days during SCAR-B, however, when assumptions about ω_0 have to be made and also when τ_s was significantly higher, the differences can be as large as 100 W m^{-2} . At TOA, the SWARF per unit optical thickness ranges from -20 to -60 W m^{-2} over four major ecosystems in South America. The results show that τ_s and ω_0 are the two most important parameters that affect DSWI calculations. For SWARF values, surface albedos also play an important role. It is shown that ω_0 must be known within 0.05 and τ_s at $0.55 \mu\text{m}$ must be known to within 0.1 to estimate DSWI to within 20 W m^{-2} . The methodology described in this paper could serve as a potential strategy for determining DSWI values in the presence of aerosols. The wavelength dependence of τ_s and ω_0 over the entire shortwave spectrum is needed to improve radiative transfer calculations. If global retrievals of DSWI and SWARF from satellite measurements are to be performed in the presence of biomass-burning aerosols on a routine basis, a concerted effort should be made to develop methodologies for estimating ω_0 and τ_s from satellite and ground-based measurements.

1. Introduction

Biomass burning is considered to be a major source of trace gas species and aerosol particles (Andreae 1991; Crutzen and Andreae 1990; Setzer and Perreira 1991).

More than 114 Tg of smoke are produced per year in the Tropics, which accounts for about 80% of the biomass that is burned globally (Hao and Liu 1994; Penner et al. 1992). The smoke aerosols can extend over large areas (Hsu et al. 1996; Herman et al. 1997; Husar et al. 1997). These aerosols affect the radiative energy budget on both regional (Christopher et al. 1998) and global scales (Penner et al. 1992). Most studies to date have examined the impact of biomass-burning aerosols at the top of the atmosphere (TOA). For example, using a

Corresponding author address: Sundar A. Christopher, Dept. of Atmospheric Sciences, 977 Explorer Blvd., University of Alabama in Huntsville, Huntsville, AL 35899.
E-mail: sundar@atmos.uah.edu

radiative transfer equation valid for optical depths less than 0.5, the global TOA radiative impact of biomass-burning aerosols has been estimated (Penner et al. 1992; Chylek and Wong 1995; Hobbs et al. 1997). Using satellite data and radiative transfer models, the impact of individual plumes (Anderson et al. 1996) and regional radiative impacts have also been computed (Christopher et al. 1996; Ross et al. 1998). Using observations and models, a reduction of surface temperatures caused by smoke from forest fires has also been reported (Robock 1988; Westphal and Toon 1991). Because of the various assumptions involved in these techniques, uncertainties continue to exist on the radiative impact of biomass-burning aerosols (Houghton et al. 1996). The TOA radiative energy budgets provide important information on regional and global climate; equally important are the radiative energy budgets at the surface. Calculations of surface and atmospheric energy budgets in biomass-burning areas have been largely hampered because of inadequate information on aerosol physical and chemical properties. Lenoble (1991) has provided a review of the radiative processes associated with smoke from biomass burning. The Smoke Clouds and Radiation—Brazil (SCAR-B) experiment (Kaufman et al. 1998), conducted during the 1995 biomass-burning season in Brazil, provided a wide variety of data relevant to the radiative impact of aerosols on the earth–atmosphere system. The current paper uses aircraft and ground-based data from SCAR-B to examine the downward shortwave irradiance (DSWI) and TOA shortwave aerosol radiative forcing values (SWARF) in biomass-burning regions.

DSWI is an important component of the radiation balance at the earth's surface and is linked with the hydrological cycle through dynamic and thermodynamic processes. Current techniques for estimating DSWI involve either radiative transfer calculations coupled with satellite data (Whitlock et al. 1995; Li 1995, 1998; Charlock and Alberta 1996) or measurements made at the surface (Gilgen and Ohmura 1999). Although surface measurements serve as important validation tie-points, their spatial sampling is generally inadequate for climate studies. Moreover, a majority of these data are usually available only as daily and monthly averages, which makes detailed validation efforts difficult. Characterizing aerosols in radiative transfer models continues to be a challenge because of 1) the diversity of aerosol types, 2) the difficulty in routinely determining aerosol spatial distributions, and 3) inadequate information about the microphysical and radiative properties of aerosols. Using the Surface Radiation Budget (SRB) product generated from the Earth Radiation Budget Experiment (Barkstrom et al. 1989) and the International Satellite Cloud Climatology Project data over $280 \text{ km} \times 280 \text{ km}$ grid cells (Schiffer and Rossow 1983), Konzelmann et al. (1996) estimated that the *monthly mean* measured values of DSWI are smaller than the calculated values by about 25%–40% in biomass-burning ar-

reas over Africa. They concluded that the differences are largely due to the inadequate characterization of biomass-burning aerosols in the SRB dataset. A recent study by Li (1998) showed that a zonal comparison between satellite-based and surface-observed surface radiation budget parameters was in good agreement except in tropical regions where biomass burning is prevalent. Most studies to date have inferred the surface effects of aerosols by comparing the observed radiation budget parameters to calculated values on a monthly mean basis (Konzelmann et al. 1996; Li 1998). The major reason for this approach is the lack of information on the optical and radiative properties of aerosols. One of the few studies to attempt DSWI calculations on an instantaneous basis was by Charlock and Alberta (1996) over the southern Great Plains region in Oklahoma. This study was performed over a well-instrumented midlatitude summertime region for clear and cloudy conditions. Their study showed that clear-sky biases on the order of 30 W m^{-2} exist between measured and calculated values. They also concluded that the bias is probably regional and is due to the inadequate characterization of aerosols and gaseous absorption. Although these biases exist from the Charlock and Alberta study, no clear-sky biases have been reported from other studies in the tropical Pacific (Chou and Zhao, 1997; Waliser et al. 1996).

The focus of the current study is to examine the impact of biomass-burning aerosols during SCAR-B at both the surface and TOA. Using in situ and ground-based measurements, four-stream radiative transfer calculations are performed to compute DSWI values over cloud-free regions. These calculations are then compared with broadband pyranometer measurements made at the surface. Using the same set of measurements, the impact of aerosols is estimated at TOA for four different ecosystems. This study differs from previous efforts in two main respects: 1) it specifically focuses upon the calculation of shortwave irradiance over biomass-burning regions in South America and 2) it uses available in situ and ground-based measurements to test and to validate the calculations. Note that these calculations are performed at specific time periods during the day and therefore are termed “instantaneous DSWI.” No temporal averaging is performed on the datasets.

2. Datasets and area of study

Several datasets are used in this study, including aerosol microphysical properties from the University of Washington Convair 131-A (UW C-131A) research aircraft, aerosol optical thickness from ground-based sun-photometer measurements, and DSWI measurements from broadband Eppley Laboratory, Inc., pyranometers at the surface. This study is limited to seven days because of the availability of surface broadband irradiance measurements from SCAR-B. A brief description of the datasets follows.

a. Aerosol optical thickness from sunphotometer measurements

Total column smoke optical thickness (τ_s) has been estimated by Holben et al (1996) for SCAR-B using direct sun measurements from the automated ground-based sun sky-scanning spectral radiometer (sunphotometer) from several sites. Direct sun measurements were made at 340, 380, 440, 500, 670, 870, and 1020 nm, and these data are converted to τ_s and Ångström wavelength exponent α , and the measurements at 940 nm are inverted to precipitable water PW (Holben et al. 1998). The τ_s values are checked carefully for cloud contamination by removing all values of the wavelength exponent that are below 1.0. (because cirrus clouds commonly have values ranging between 0 and 0.5). An average of three observations (triplet) is made at 30-s intervals, and this measurement sequence is repeated every 15 min. For each observation, a triplet percentage variation is first computed. Assuming that the variability of clouds is larger than that of aerosols, all data with a triplet range of 0.02 in τ_s or $0.03\tau_s$ (whichever is greatest) are eliminated.

b. UW C-131A in situ measurements

During SCAR-B, the UW C-131A research aircraft made 29 flights in Brazil (~90 flight hours) and a wide variety of data were collected (Hobbs 1996). Of particular importance to this study are 1) vertical profiles of temperature and water vapor, 2) derived values of the single-scattering albedo ω_0 , and 3) vertical profiles of light-scattering and light-absorption coefficients of smoke aerosols. The top altitudes of most C-131A measurements are about 4.5 km, and the vertical resolution of the C-131A measurements could be as high as 20 m. The light-scattering coefficient was measured with a three-wavelength ($\lambda = 450, 550, \text{ and } 700 \text{ nm}$) integrating nephelometer, and the light-absorption coefficient was measured at a wavelength of 550 nm (Reid et al. 1998a) using two methods. Teflon filters were exposed to measured volumes of ambient air, and the results were analyzed using the integrating plate method. In the second technique, ambient air was pumped through a filter, and the attenuation of light is measured with a particle and soot absorption photometer. The measured light scattering was further corrected to the ambient relative humidity (Kotchenruther and Hobbs 1998). The ratio of the light-scattering and light-extinction coefficients provides single-scattering albedo values. Aerosol size distributions were measured continuously with a suite of three optical particle spectrometer probes mounted externally on the aircraft. The smoke particles were approximated as spheres (Martins et al. 1998) consisting of a refractory, absorbing core of black carbon surrounded by a nonabsorbing shell of unspecified organic compounds and sulfates (Reid et al. 1998b). Using Mie calculations, the measured particle

size distributions and estimates of the bulk chemical composition were used to obtain the mass concentrations of particles and their scattering and absorption coefficients (Reid et al. 1998a). These values were then compared to the direct measurements made simultaneously aboard the aircraft using the filters, integrating nephelometer, and absorption photometer. Internal closure calculations show that the calculated light scattering and mass concentrations were within 20% of the directly measured values, and the differences probably are due to uncertainties in measurements and inadequacy of standard Mie calculations. Further details of the techniques can be found in Reid et al (1998a) and Kotchenruther and Hobbs (1998).

c. Eppley pyranometer measurements

Precision spectral pyranometer (PSP) instruments were used in SCAR-B to measure the incident total (direct plus diffuse) irradiance on a horizontal surface on the ground (Eck et al. 1998). These instruments measure DSWI between 0.28 and 2.8 μm . The Eppley Laboratory calibrated the instruments, which were within $\pm 1\%$ of the World Radiation Reference. In addition, two PSP pyranometers operated side by side on the roof of the Instituto Nacional de Pesquisas Espaciais laboratory in Cuiaba, Brazil, for 5 h (sampled at 1-min intervals) on 27 August 1995. The DSWI values measured by these two instruments in this time period agreed with each other to within 1.3%.

During SCAR-B, the temporal variability of the measurements was taken at 1-min or 5-min intervals depending upon the location. High-frequency temporal variation, or decreasing (increasing) irradiance with decreasing (increasing) solar zenith angle, was identified as being due to clouds. During this time, the incident photosynthetically active radiation between 0.4 and 0.7 μm was also measured. Because the ratio of PAR to total irradiance is influenced by the presence of both aerosols and clouds, cloud contamination was detectable by evaluating the time series of the PAR-to-total irradiance ratio. Higher values of the ratio represent cloud conditions from absorption by water vapor in the near infrared, and lower values of the ratio represents high aerosol loading from higher aerosol optical depths at shorter wavelengths (Pinker and Laszlo 1992a). A third test for cloud contamination was made by examining the wavelength variation of the aerosol optical thickness. For biomass-burning aerosols in Brazil, the Ångström wavelength exponent typically varies from 1.6 to 2.0, with values lower than 1.6 resulting from cloud contamination from the large size of water droplets and ice crystals in clouds (Holben et al. 1996). When all three of these cloud-screening tests were passed for at least a 1-h interval, the data were identified as being cloud free. Further details can be found in Eck et al (1998).

Figure 1 shows the area of study and the locations of

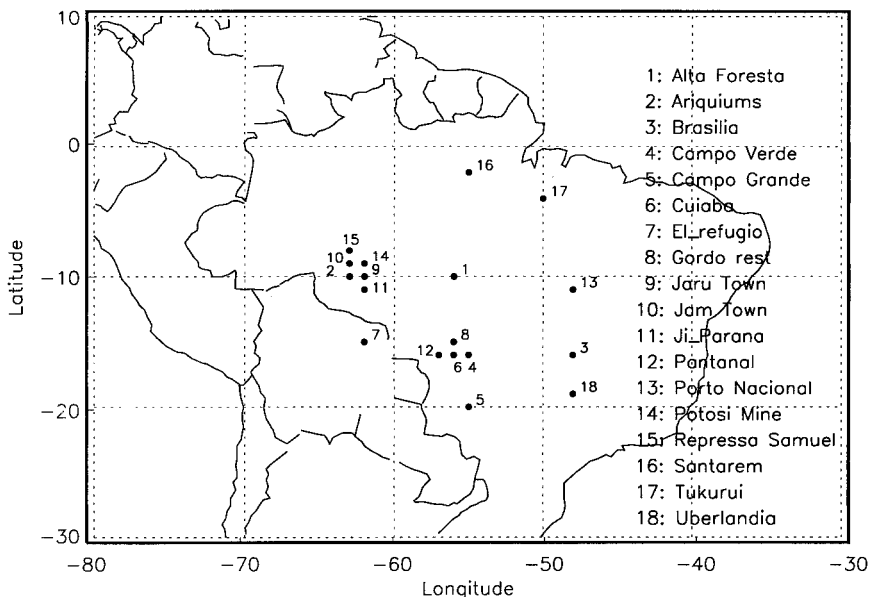


FIG. 1. Area of study and sunphotometer sites during SCAR-B.

the sunphotometers during SCAR-B (Kaufman et al. 1998). Table 1 lists the case studies that are examined here. The three sites at which the Eppley pyranometer measurements were made were:

- 1) Cuiaba (15°S, 56°W) on 27 August and 1 September 1995,
- 2) Potosi Mine (9°S, 63°W) on 4–7 September 1995, and
- 3) Pantanal (16°S, 56°W) on 30 August 1995.

Potosi Mine, which is located in the state of Rondonia in Brazil, was a site of intense burning as seen by the fire patterns observed from Geostationary Operational Environmental Satellite (Prins et al. 1998; Christopher et al. 1998). Dense smoke with optical thickness greater than 2 (at 0.55 μm) was often measured at this site during SCAR-B. Cuiaba and Pantanal are located on the southern border of the Amazon watershed in a cerrado region, which is primarily use for agricultural cultivation and is downwind of the intense burning areas. Coincident sunphotometer measurements were also made

at the aforementioned sites during this time period. On 27 August 1995, the C-131A aircraft (UW flight No. 1694) made measurements (15.5°S, 56°W) between 1633 and 2027 UTC in Cuiaba, and on 1 September 1995 (UW flight No. 1697) it made measurements between 1206 and 1445 UTC southwest of Cuiaba near Pantanal. These two days are considered to be “control cases,” for which near-coincident measurements were available from ground-based and airborne in situ measurements. Five other days (30 August and 4–7 September 1995) are considered “validation cases,” for which only sunphotometer measurements and surface-based Eppley pyranometer measurements were available.

3. Radiative transfer model

a. Description

A delta-four-stream plane-parallel broadband radiative transfer model (Fu and Liou 1993) was used to

TABLE 1. Details of locations and times for the case studies. See Fig. 1 for location of sites. Surface measurements denote both the sunphotometer and the Eppley pyranometer measurements.

No.	Location	Date in 1995 (MM/DD)	C131-A flight No.	C-131A profile time (UTC)	Surface measurements (UTC)
1	Cuiaba	08/27	1694 (Cuiaba)	1633–2027	1500–2000
2	Cuiaba	09/01	1697 (Pantanal)	1206–1445	1300–1430
3	Pantanal	08/30	Not applicable	Not applicable	1200–1800
4	Potosi Mine	09/04	Not applicable	Not applicable	1200–2000
5	Potosi Mine	09/05	Not applicable	Not applicable	1200–2000
6	Potosi Mine	09/06	Not applicable	Not applicable	1600–1800
7	Potosi Mine	09/07	Not applicable	Not applicable	1300–1600

compute DSWI values in the presence of biomass-burning aerosols. In previous research, this model has been used to calculate TOA, surface, and atmospheric fluxes in clear and cloudy (water and ice clouds) conditions (e.g., Fu and Liou 1993; Charlock and Alberta 1996). In the current study, this model is modified to account for biomass-burning aerosols by utilizing measured aerosol properties from the C131A aircraft and τ_s from the sunphotometer measurements. The delta-four-stream approach agrees with adding-doubling calculations to within 5% for fluxes and is an improvement over the two-stream approach (Liou et al. 1988). In this model, the correlated- k distribution is used for gaseous absorption and emission. The gases considered in the model include H_2O , CO_2 , O_3 , O_2 , CH_4 , and N_2O . The radiative effects of Rayleigh scattering, liquid water droplets, ice crystal, continuum absorption of H_2O , and surface albedo are considered. In this model, the shortwave (SW) spectrum (0.2–4.0 μm) is divided into 6 bands: 0.2–0.7, 0.7–1.3, 1.3–1.9, 1.9–2.5, 2.5–3.5, and 3.5–4.0 μm . For the principal atmospheric gases, the four-stream approach matches line-by-line simulations of fluxes to within 0.05% for SW calculations. Note that the Eppley PSP measures DSWI values between 0.28 and 2.8 μm , whereas the SW bands in the radiative transfer model extend up to 4.0 μm . Therefore, only the first four bands in the radiative transfer model are used in the comparison. The input parameters required for SW calculations include:

- 1) atmospheric profiles of water vapor, O_3 , temperature, and pressure;
- 2) ω_0 and asymmetry parameter g in the SW bands along with vertical profiles of these aerosol properties;
- 3) τ_s at these wavelengths;
- 4) surface albedos for the shortwave bands; and
- 5) solar zenith angle.

The output parameters include upwelling and downwelling fluxes in each of the prescribed 28 layers, from which the radiative fluxes at TOA and at the surface can be obtained. The surface albedo in the six SW bands for Cuiaba and Pantanal was assumed to be as follows: 0.12, 0.31, 0.34, 0.34, 0.34, and 0.34, which are representative of the cerrado ecosystem (Charlock 1997). For Potosi Mine, the surface type is assumed to be forest, for which the corresponding surface albedos were assumed to be 0.04, 0.20, 0.20, 0.20, 0.20, and 0.20, respectively. The sensitivity of the results to this assumption is examined in section 4b. For the control cases, vertical profiles of temperature and water vapor were obtained from the C-131A aircraft measurements along with tropical ozone profiles (McClatchey et al. 1972). For the validation cases, standard tropical water vapor and temperature profiles are used (McClatchey et al. 1972). For both the validation and control cases, the smoke aerosols are assumed to be in the lowest 4 km (Reid et al. 1998b). Between 4 and 12 km a continental

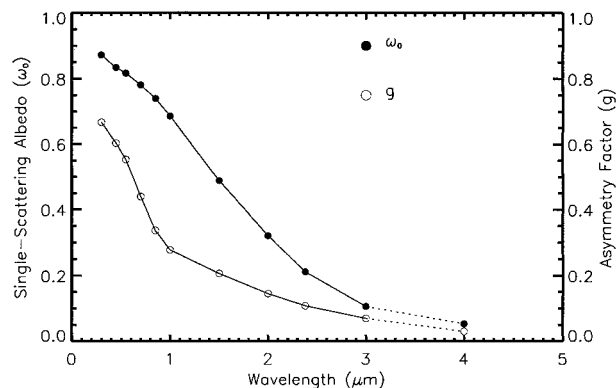


FIG. 2. Wavelength dependence of the single-scattering albedo ω_0 (solid circles) and asymmetry parameter g (open circles). Dotted lines indicate extrapolation.

aerosol model is used, and between 12 and 25 km a stratospheric aerosol model is assumed.

b. Characterization of smoke aerosols

One of the standard techniques for computing the radiative properties of aerosols is to assume an aerosol size distribution and refractive index, which are then used as input to Mie calculations (e.g., Kaufman and Nakajima 1993; Anderson et al. 1996; Lenoble 1991). The aerosol particles are assumed to be spherical (Martins et al. 1998), and Mie calculations are performed, which provide the phase function, ω_0 , g , and extinction coefficients. These values are then used to compute the TOA and surface irradiance values. However, it is often difficult to obtain the required aerosol microphysical and chemical information (size distribution, refractive index) to use in Mie calculations. Therefore, climatological values are often assumed that may not be representative for biomass-burning aerosols. In the current study, a different approach is used to compute the radiative effects of smoke aerosols. The smoke radiative effect is specified by the τ_s values, ω_0 , and the phase function for smoke. The optical thickness of the smoke is obtained from ground-based sunphotometer measurements, and ω_0 values are obtained from in situ measurements in Brazil (see section 2b).

The four-stream broadband radiative transfer model requires ω_0 and g between 0.2 and 4.0 μm in six discrete intervals. For the sake of completeness, the calculations are performed in all six SW bands, although the comparison with the Eppley pyranometer requires only the first four bands from the radiative transfer model. Using fine-mode calculations for biomass-burning aerosol particles, wavelength-dependent ω_0 and g values are produced between 0.3 and 3.0 μm (Ross et al. 1998), and the values are extrapolated to 4.0 μm (as shown by the dotted lines in Fig. 2). Figure 2 shows the ω_0 and g values used in the radiative transfer calculations. Both ω_0 and g decrease with increasing wavelength. For ex-

ample, from Fig. 2, ω_0 is 0.823 (at $0.55 \mu\text{m}$) with values decreasing to about around 0.053 at $4 \mu\text{m}$. The values of g range from about 0.553 at $0.55 \mu\text{m}$ to about 0.030 at $4 \mu\text{m}$. Based on Fig. 2, the energy-weighted values of ω_0 and g for each band are used as input to the four-stream model (Pinker and Laszlo 1992b). Similarly, the measured aerosol optical thickness at each site is weighted by the incoming solar energy for each band and is used in the radiative transfer calculations.

For the water-soluble aerosols, including the smoke particles, the light-scattering coefficient σ_s increases as ambient relative humidity RH increases. The *humidification factor*, which is a measure of this increase, is defined as σ_s at 80% RH divided by σ_s of the dry aerosol (Kotchenruther and Hobbs 1998). The σ_s of smoke particles from various types of fires as a function of RH were estimated from these measurements and the single-scattering albedos used in the calculation account for this humidification factor.

The basic strategy is as follows:

- 1) For the two control cases over Cuiaba (27 and 30 August), for which near-coincident C-131A airborne and sun photometer measurements are available, DSWIs are computed from the radiative transfer model, and the results are compared with the broadband pyranometer measurements made at the surface.
- 2) For the five validation cases, for which C131-A measurements were not available, average values of ω_0 and g (from six selected flights), along with standard tropical water vapor and ozone amounts, are assumed. These values then are used in the radiative transfer calculations to compute DSWI. The calculated values are then compared with the ground-based pyranometer measurements.

We use this approach because it allows us to address the following questions. In a data-rich environment (e.g., SCAR-B), how well can we estimate DSWI from radiative transfer calculations? How do these calculations compare with the surface-based measurements? Can we use field experiment data to obtain "average" values of aerosol properties that are applicable to satellite-based algorithms? For example, after a pixel is labeled as "smoke" from satellite imagery, radiative transfer models are required to compute the effects of aerosols (Charlock and Alberta 1996). To perform these calculations, knowledge of the microphysical properties of the smoke is necessary. This study is a first step toward examining the importance of various aerosol properties on DSWI and TOA calculations.

4. Results and discussion

a. Comparison between measured and calculated DSWI values

For the two control cases, the observed DSWI from the Eppley pyranometer; column optical thickness at

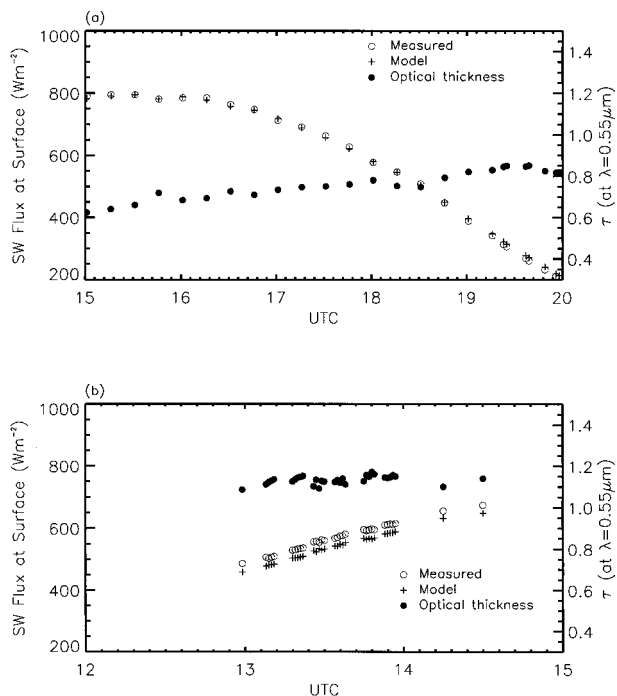


FIG. 3. Comparison between measured (open circles) and calculated (+ signs) DSWI for (a) 27 Aug 1995 and (b) 1 Sep 1995 over Cuiaba as a function of UTC time. Also shown in solid circles is the measured aerosol optical thickness at $0.55 \mu\text{m}$.

seven wavelengths from the sunphotometer; profiles of temperature, pressure, dewpoint temperature, potential temperature, and smoke extinction coefficient; and vertical profiles of ω_0 are available. However, for 1 September 1995, the in situ measurements are from Pantanal, which is about 100 km from Cuiaba.

Figures 3a,b show the calculated values of DSWI from the four-stream radiative transfer model and the observed DSWI from the Eppley pyranometer for 27 August and 1 September 1995 over Cuiaba. The open circles represent the measured DSWI values and the "+" symbols denote the model-calculated values. Also shown, by the solid circles, are the measured values of τ_s at $0.55 \mu\text{m}$. Figure 3a shows the DSWI values changing from 800 to about 200 W m^{-2} from 1500 to 2000 UTC over Cuiaba on 27 August. Note that, on this day, the C-131A measurements were made between 1633 and 2027 UTC. Six overpasses were made over the sunphotometer, and uniform thick smoke was observed during the time of the C131-A measurements (Kaufman et al. 1998). During this day, fires and smoke were also observed from satellite measurements over much of this region (Prins et al. 1998). Figure 3a shows that, during this time, the sunphotometer measured τ_s ($0.55 \mu\text{m}$) values (solid circles) that varied from 0.6 to 0.8, with peak values between 1900 and 2000 UTC. The calculated DSWI values are in excellent agreement with the pyranometer measurements for this day over Cuiaba. The root-mean-square (rms) difference between ob-

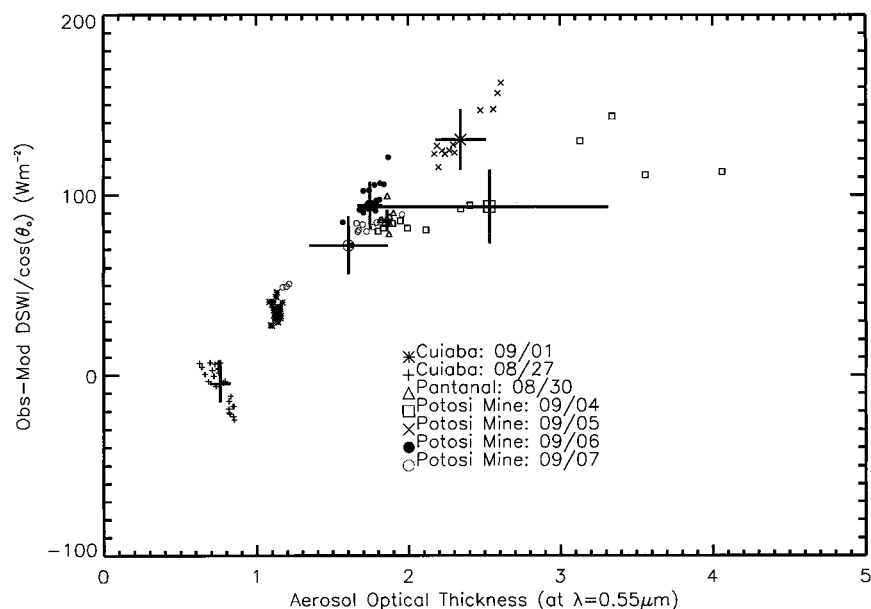


FIG. 4. Normalized differences between measured and calculated values as a function of aerosol optical thickness for all case studies. Large crosses indicate std dev.

served and calculated values for 25 sets of measurements is 6.2 W m^{-2} for 27 August, and the bias error (observed - calculated) is -1.9 W m^{-2} . Figure 3b shows similar results over Cuiaba for 1 September 1995. The C-131A measurements were made between 1206 and 1445 UTC, when a thick uniform haze was present (Prins et al. 1998). The sunphotometer and Eppley cloud-free measurements are available only between 1300 and 1430 UTC. Note the consistently large aerosol optical thickness values around 1.15 as compared with Fig. 3a. For the 33 instantaneous measurements on 1 September 1995, the DSWI values are between 500 and 650 W m^{-2} . The rms error between the measured and calculated values is 27.4 W m^{-2} , and the bias error is 27.3 W m^{-2} . From these two cases, it is inferred that, given adequate information about the optical and radiative properties of biomass-burning aerosols, the DSWI values can be calculated to within 30 W m^{-2} . The differences between the measurements and calculations probably are due to temporal lack of collocation between the UW C-131A measurements and the sun-

photometer measurements, assumptions concerning the wavelength dependency of ω_0 and g , and, the assumption that the C131-A measurements made during a particular time are representative of the entire time period.

For the validation cases, only the observed τ_s and the DSWI measurements are available. Therefore, average values of ω_0 and g are used to calculate the DSWI from the four-stream radiative transfer model. The reason for this approach is to determine if average values of aerosol properties are adequate for DSWI calculations. Standard water vapor, temperature, and ozone profiles for the tropical atmosphere are assumed. The average value of ω_0 at $0.55 \mu\text{m}$ is 0.823, and g is 0.553; the wavelength dependence of these values is shown in Fig. 2. Figure 4 shows the relationship between observed-minus-calculated DSWI values as a function of the measured τ_s at $0.55 \mu\text{m}$ for all the seven days, which include both the control and the validation cases. Also shown in Fig. 4 are the standard deviations in τ_s and the DSWI values. Table 2 shows the rms errors for each day. The measured τ_s ($0.55 \mu\text{m}$) ranges from 0.5 to 2.6 over these sites. As τ_s increases, the differences between the measured and calculated values get larger, with a limiting value of about 150 W m^{-2} . For the two control cases (27 August, 1 September) over Cuiaba for which single-scattering albedo values were available from in situ measurements, the rms errors are 6.17 and 27.43 W m^{-2} , respectively. For five days when measured values of ω_0 and g were not available, average values were used. The differences between measured and calculated DSWI are a linear function of aerosol optical thickness. As τ_s (at $0.55 \mu\text{m}$) increases, the rms errors also increase. In section 4b we show that to decrease the differences between

TABLE 2. Bias (observed - calculated) (W m^{-2}) and root-mean-square errors (W m^{-2}) for the study.

Location	Date	Mean τ_s ($0.55 \mu\text{m}$)	Rms error	Bias
Cuiaba	27 Aug 1995	0.76	6.17	-1.86
Cuiaba	2 Sep 1995	1.13	27.43	27.29
Pantanal	30 Aug 1995	1.86	69.50	69.44
Potosi Mine	4 Sep 1995	2.54	67.90	65.78
Potosi Mine	5 Sep 1995	2.34	113.82	111.11
Potosi Mine	6 Sep 1995	1.75	80.87	77.60
Potosi Mine	7 Sep 1995	1.60	54.51	52.08

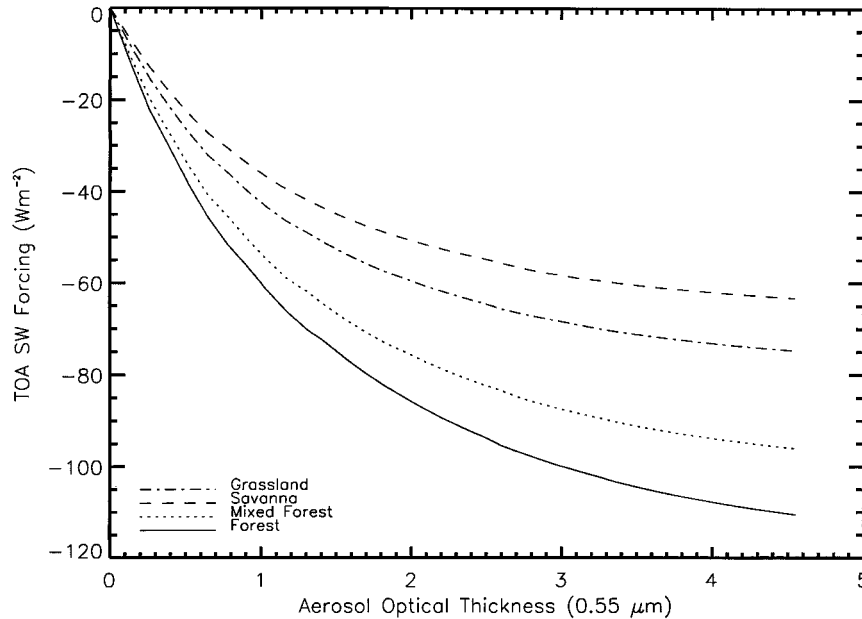


FIG. 5. The SWARF values at the top of the atmosphere for four different ecosystems as a function of aerosol optical thickness.

measured and calculated values the aerosols would have to be less absorptive (i.e., larger ω_0 values), which would increase the DSWI. The strategy of assuming average aerosol ω_0 values may not be suitable for radiative transfer studies.

Next we examine the effect of biomass-burning aerosols at TOA from radiative transfer calculations. Unfortunately, no broadband measurements were made at TOA to validate the results. The difference between clear and aerosol conditions is defined as SWARF (Christopher et al. 1998). The results shown in Fig. 5 are for four major ecosystems in Brazil. The four different ecosystems and their corresponding broadband shortwave clear-sky albedos are 1) forest (10.6%), 2) mixed forest (12.9%), 3) savanna (16.6%), and 4) grassland (14.9%). The SWARF results are shown as a function of aerosol optical thickness at $0.55 \mu\text{m}$. These calculations are performed at a solar zenith angle of 45° for a tropical atmosphere. The ω_0 values are assumed to be 0.88 for all ecosystems and are average conditions for regional and aged smoke (Reid et al. 1998b). The wavelength dependence of single-scattering albedo is obtained from Fig. 2. As τ_s increases, SWARF also increases because of the increased reflection from aerosols. For a unit change in aerosol optical thickness (from 0 to 1), the change in SWARF for the forest, mixed forest, savanna, and grassland ecosystems is about -60 , -55 , -37 , and -43 W m^{-2} . This change in SWARF for a unit change in aerosol optical thickness could be different for different solar zenith angles and values of the assumed single-scattering albedo and surface albedo. For a given ecosystem, the change in SWARF at TOA is strongly dependent upon the assumed surface albedo.

As τ_s changes from 1 to 2, SWARF changes at a much slower rate.

b. Sensitivity of calculated DSWI to aerosol and ambient parameters

To understand the differences between the measured and calculated DSWI values, we will now examine the sensitivity of several model parameters to DSWI using the four-stream radiative transfer calculations. The following model parameters are examined: 1) aerosol optical thickness, 2) single-scattering albedo, 3) asymmetry parameter, 4) surface albedo, 5) column water vapor amount, and 6) column ozone amount.

As a first test, the sensitivity of DSWI to a range of aerosol optical thickness at $0.55 \mu\text{m}$ is examined as a function of solar zenith angle. To perform these calculations, ω_0 , surface albedo, g , column water vapor, and ozone amounts are fixed. The column ω_0 (at $0.55 \mu\text{m}$) for smoke aerosols between 0 and 4 km is assumed to be 0.823, and the column g value is 0.55. By varying the τ_s values while holding all other parameters constant, the sensitivity of the DSWI values to τ_s can be estimated. Figure 6a shows that the calculated values of DSWI are extremely sensitive to the assumed values of τ_s . As τ_s increases at a given solar zenith angle θ_0 , the amount of SW energy at the surface decreases. Also, for a constant value of τ_s , a larger solar zenith angle produces lower DSWI values. For example, at $\theta = 31.7^\circ$ [$\cos(\theta_0) = 0.85$], as τ_s varies from 0.5 to 1.0, the DSWI value changes from 750 to 600 W m^{-2} . The radiative transfer calculations show that an uncertainty of 0.1 in τ_s (and for the range of smoke optical thickness and

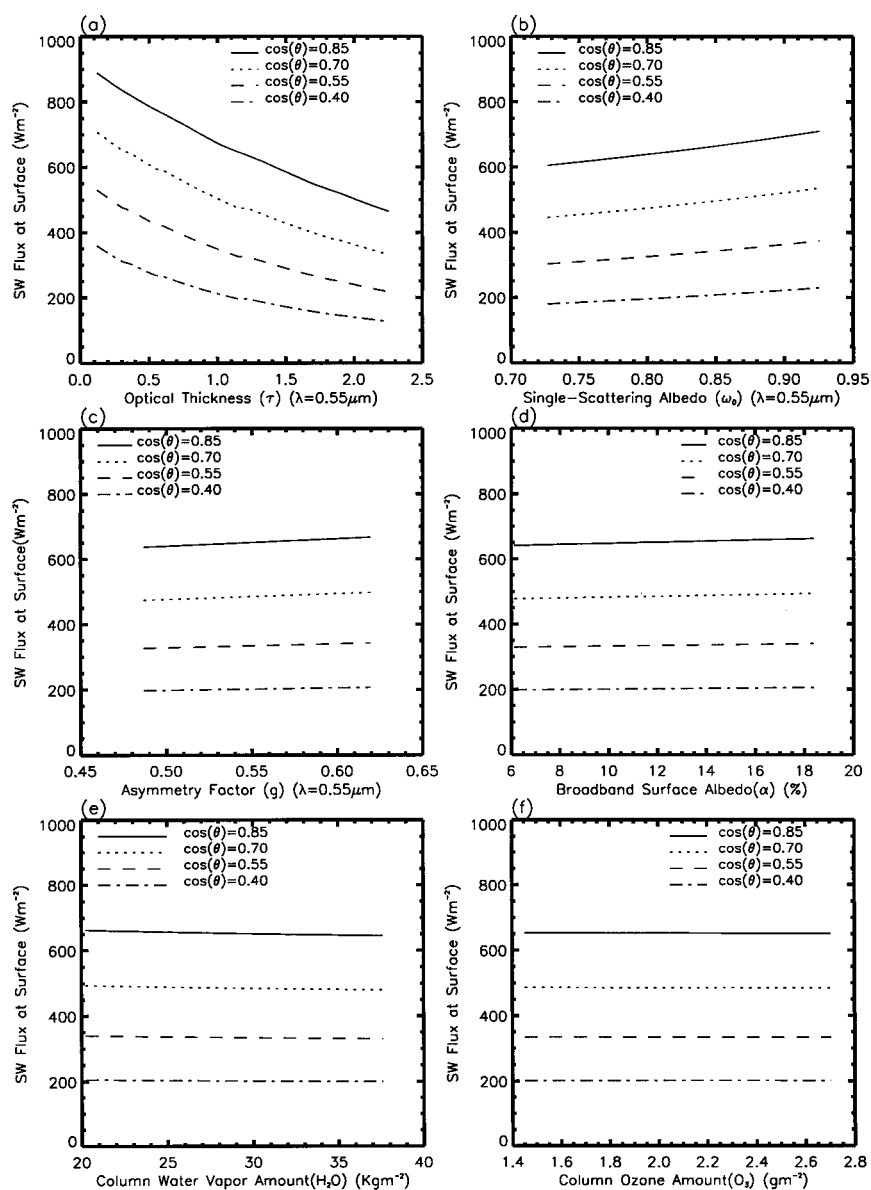


FIG. 6. Sensitivity of calculated DSWI to (a) aerosol optical thickness, (b) single-scattering albedo, (c) asymmetry parameter, (d) surface albedo, (e) column water vapor, and (f) column ozone amount.

solar zenith angles that are considered here) will yield an uncertainty of about $20\text{--}30\text{ W m}^{-2}$ in DSWI, assuming that all other variables (e.g., g , ω_0) are known. Figure 6b shows the sensitivity of the calculated DSWI values to ω_0 at different solar zenith angles. The column τ_s is assumed to be 0.95 at $0.55\text{ }\mu\text{m}$. For a given θ_0 , as ω_0 increases, the DSWI values increase from the scattering, which is predominantly in the forward direction. At a θ_0 of 31.7° , a change in ω_0 between 0.80 and 0.85 produces an increase in DSWI of about 25 W m^{-2} . Figures 6c–f show only small changes in DSWI as g , surface albedo, column water vapor, and column

ozone are varied. A change in g of 10% (between 0.55 and 0.60) produces a change in DSWI of less than 10 W m^{-2} . A 40% change in surface albedo (from 10% to 14%) produces a DSWI change of less than 10 W m^{-2} . Similar changes can be seen in Figs. 6e,f when column water vapor and column ozone values are changed. From Fig. 6 we conclude that the DSWI calculations are sensitive primarily to the assumed values of τ_s and ω_0 . Both τ_s and ω_0 must be estimated to within 10%–12% to obtain DSWI values within 20 W m^{-2} , which means that τ_s and ω_0 must be estimated to within 0.1 and 0.05, respectively. Therefore, if global retrievals of

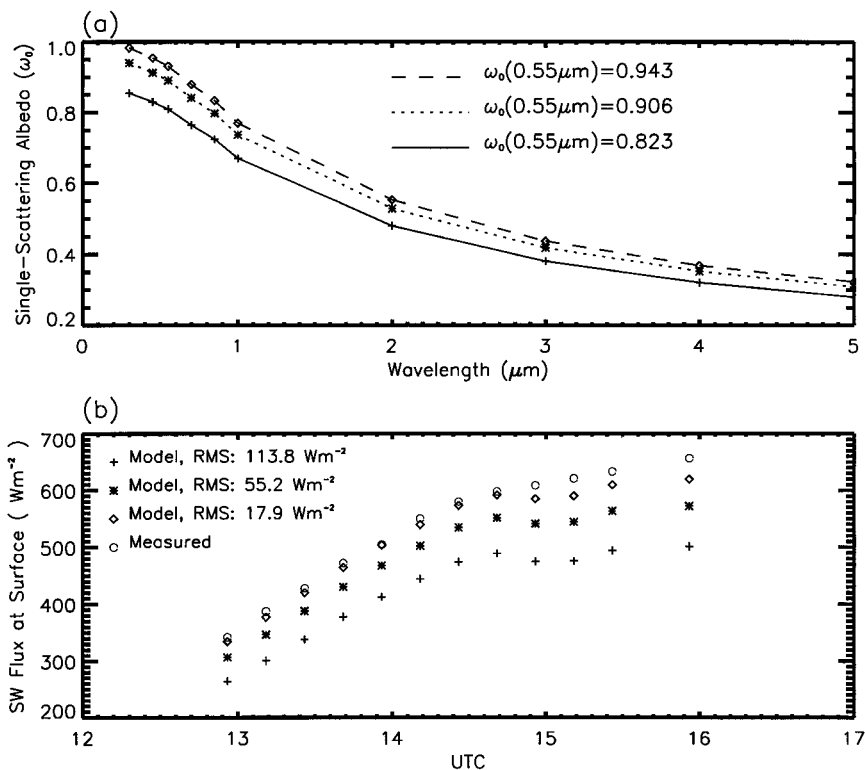


FIG. 7. Tuning single-scattering albedo to match measured and calculated values for Potosi Mine on 5 Sep 1995: (a) wavelength dependence of the single-scattering albedo and (b) calculated DSWI values.

DSWI are to be done on a routine basis using satellite and radiative transfer calculations, new methodologies must be developed to estimate τ_s and ω_0 accurately.

Having determined that τ_s and ω_0 are the two major parameters that affect the calculation of DSWI, we will now further examine the data from Potosi Mine on 5 September 1995, for which the rms errors between the measured and calculated values were the largest (113.8 W m^{-2} ; see Table 2). Because the τ_s values are obtained from sunphotometer measurements that have a small uncertainty (~ 0.01), we will assume that ω_0 is the only variable that needs to be adjusted to reduce the rms errors, because the other variables, as shown in Fig. 6, play a minor role. Figure 7a (solid line) shows the ω_0 values at $0.55 \mu\text{m}$ as a function of wavelength that produced an rms error of 113.8 W m^{-2} . The DSWI values at the surface corresponding to this set of ω_0 values are shown in Fig. 7b (as the “+” symbols). Because the model underestimates the DSWI values, the ω_0 values need to be increased (to make the aerosols less absorptive and to increase scattering to produce higher DSWI values at the surface). We will adjust the entire ω_0 curve, instead of changing the value at a particular wavelength. Figure 7a (dotted lines) shows the results of a 10% increase (from 0.823 to 0.906) in ω_0 , and in Fig. 7b the “*” symbols show the corresponding changes in DSWI values; the rms errors decreased from

113.8 to 55.2 W m^{-2} . A 15% increase in ω_0 (from 0.823 to 0.943) results in a decrease of rms errors from 113.8 to 17.9 W m^{-2} . This is an extreme case in which the rms errors were large (113.8 W m^{-2}) to begin with. This range of single-scattering albedo is consistent with other SCAR-B studies (e.g., Dubovik et al. 1998). Although changes to ω_0 alone can reduce the rms errors between the measured and calculated DSWI values, in an operational algorithm τ_s values may at the same time also have to be adjusted to provide the desired accuracy in the estimation of DSWI values.

5. Summary

Biomass-burning aerosols play a significant role in modulating the radiative energy budgets on both regional and global scales. Characterizing biomass-burning aerosols in radiative transfer models is generally difficult because of inadequate information on aerosol microphysical properties such as optical depth and single-scattering albedo. During the SCAR-B 1995 field campaign in Brazil, detailed measurements were obtained on aerosol microphysical properties from the UW C-131A aircraft and from ground-based sunphotometer measurements. In this study, we have used a four-stream radiative transfer model to calculate the downward shortwave irradiances for two days over Cuiaba, where

near-coincident aircraft and sunphotometer measurements were available. The calculated DSWI values have been compared with broadband Eppley pyranometer DSWI measurements at the surface. For these two cases, it is shown that the rms differences between the calculated and measured DSWI values are less than 30 W m^{-2} . However, when single-scattering albedo values had to be assumed (rather than measured), the rms ranged from 55 to 114 W m^{-2} . The difference between measured and calculated values increases as the optical thickness increases. If one assumes a “wrong” single-scattering albedo, then as the total optical thickness increases the error in the scattering optical thickness will also increase, which, in turn, leads to an increase of the error in the irradiance at the surface. We conclude that ω_0 must be known to within 0.05 and τ_s must be known to within 0.1 to estimate DSWI to within 20 W m^{-2} . When aerosol optical thickness data are available, a simple first-order tuning of ω_0 can reduce the rms errors from 113.8 to 17.9 W m^{-2} . This study is a first step toward understanding the surface shortwave radiative impact of biomass-burning aerosols. It also is shown that at TOA the shortwave radiative forcing per unit optical thickness is on the order of -20 to -60 W m^{-2} depending upon the solar zenith angle, surface albedo, and the assumed values of single-scattering albedo. More detailed validation studies are needed over different ecosystems, and knowledge of the wavelength dependencies of ω_0 and τ_s are necessary to improve radiative transfer calculations. Although the Aerosol Robotic Network program (Holben et al. 1998) provides continuous information on aerosol optical depth over several regions of the earth, it is equally important to measure the DSWI values over biomass-burning regions in order to validate the retrievals made from satellite measurements.

Acknowledgments. This research is partially supported by NASA Grants NAGW-5195 under NASA's New Investigator Program, NCC8-141, and NAG5-7270. Xiang Li is supported under NASA's Earth System Science Fellowship program. Sundar A. Christopher thanks Drs. Yoram J. Kaufman and Tim Suttles for their continuing encouragement. P. Hobbs was supported by the Joint Institute for the Study of the Atmosphere and the Ocean (JISAO) under NOAA Cooperative Agreement NA67RJ0155.

REFERENCES

- Anderson, B. E., and Coauthors, 1996: Aerosols from biomass burning over the southern tropical Atlantic region: Distributions and impact. *J. Geophys. Res.*, **101**, 24 117–24 137.
- Andreae, M. O., 1991: Biomass burning: Its history, use, and distribution and its impact on environmental quality and global climate. *Global Biomass Burning: Atmospheric, Climatic and Biospheric Implications* J. S. Levine, Ed., MIT Press, 3–21.
- Barkstrom, B., E. Harrison, G. Smith, R. Green, J. Kibler, R. Cess, and the ERBE Science Team, 1989: Earth Radiation Budget Experiment (ERBE) archival and April 1985 results. *Bull. Amer. Meteor. Soc.*, **70**, 1254–1262.
- Charlock, T. P., 1997: Surface and atmospheric radiation budget. *Proc. 14th CERES Science Team Meeting*, Fort Collins, CO, NASA Langley Research Center.
- , and T. L. Alberta, 1996: The CERES/ARM/GEWEX Experiment (CAGEX) for the retrieval of radiative fluxes with satellite data. *Bull. Amer. Meteor. Soc.*, **77**, 2673–2683.
- Chou, M.-D., and W. Zhao, 1997: Estimation and model validation of surface solar radiation and cloud radiative forcing using TOGA COARE measurements. *J. Climate*, **10**, 610–620.
- Christopher, S. A., D. V. Kliche, J. Chou, and R. M. Welch, 1996: First estimates of the radiative forcing of aerosols generated from biomass burning using satellite data. *J. Geophys. Res.*, **101**, 21 265–21 273.
- , M. Wang, T. A. Berendes, R. M. Welch, and S. K. Yang, 1998: The 1985 biomass burning season in South America: Satellite remote sensing of fires, smoke, and regional radiative energy budgets. *J. Appl. Meteor.*, **37**, 661–678.
- Chylek, P., and J. Wong, 1995: Effect of absorbing aerosols on global radiation budget. *Geophys. Res. Lett.*, **22**, 929–931.
- Crutzen, P. J., and M. O. Andreae, 1990: Biomass burning in the Tropics: Impact of atmospheric chemistry and biogeochemical cycles. *Science*, **250**, 1669–1678.
- Dubovik, O., B. N. Holben, Y. J. Kaufman, M. Yamasoe, A. Smirnov, D. Tanre, and I. Slutsker, 1998: Single-scattering albedo of smoke retrieved from the sky radiance and solar transmittance measured from ground. *J. Geophys. Res.*, **103**, 31 903–31 923.
- Eck, T. F., B. N. Holben, I. Slutsker, and A. Setzer, 1998: Measurements of irradiance attenuation and calculation of aerosol single scattering albedo for biomass burning aerosols in Amazonia. *J. Geophys. Res.*, **103**, 31 865–31 878.
- Fu, Q., and K. N. Liou, 1993: Parameterization of the radiative properties of cirrus clouds. *J. Atmos. Sci.*, **50**, 2008–2025.
- Gilgen, H., and A. Ohmura, 1999: The Global Energy Balance Archive. *Bull. Amer. Meteor. Soc.*, **80**, 831–850.
- Hao, W. M., and M.-H. Liu, 1994: Spatial and temporal distribution of biomass burning. *Global Biogeochem. Cycles*, **8**, 495–503.
- Herman, J. R., P. K. Bhartia, O. Torres, C. Hsu, C. Seftor, and E. Celarier, 1997: Global distribution of UV-absorbing aerosols from NIMBUS-7/TOMS data. *J. Geophys. Res.*, **102**, 16 911–16 922.
- Hobbs, P. V., 1996: Summary of types of data collected on the University of Washington's Convair C-131A aircraft in the Smoke, Clouds, and Radiation—Brazil (SCAR-B) field study from 17 August–20 September 1995. Report from the Cloud and Aerosol Research Group, Dept. of Atmospheric Sciences, University of Washington, Seattle, WA. [Available from University of Washington, Seattle, WA 98195.]
- , J. S. Reid, R. A. Kotchenruther, R. J. Ferek, and R. Weiss, 1997: Optical parameters for smoke particles in Brazil and the direct radiative forcing of climate by smoke from biomass burning. *Science*, **275**, 1776–1778.
- Holben, B. N., A. Setzer, T. F. Eck, A. Pereira, and I. Slutsker, 1996: Effect of dry-season biomass burning on Amazon basin aerosol concentrations and optical properties, 1992–1994. *J. Geophys. Res.*, **101**, 19 465–19 481.
- , and Coauthors, 1998: AERONET—A federated instrument network and data archive for aerosol characterization. *Remote Sens. Environ.*, **66**, 1–16.
- Houghton, J. T., L. G. Meiro Filho, B. A. Callander, N. Harris, A. Kattenburg, and K. Maskell, Eds., 1996: *Climate Change, 1995: The Science of Climate Change*. Cambridge University Press, 572 pp.
- Hsu, N. C., and Coauthors, 1996: Detection of biomass burning smoke from TOMS measurements. *Geophys. Res. Lett.*, **23**, 745–748.
- Husar, R. B., J. M. Prospero, and L. L. Stowe, 1997: Characterization of tropospheric aerosols over the oceans with the NOAA Advanced Very High Resolution Radiometer optical thickness operational product. *J. Geophys. Res.*, **102**, 16 889–16 909.

- Kaufman, Y. J., and T. Nakajima, 1993: Effect of Amazon smoke on cloud microphysics and albedo—analysis from satellite imagery. *J. Appl. Meteor.*, **32**, 729–744.
- , and Coauthors, 1998: Smoke, Clouds, and Radiation—Brazil (SCAR-B) experiment. *J. Geophys. Res.*, **103**, 31 783–31 808.
- Konzelmann, T., D. R. Cahoon, and C. H. Whitlock, 1996: Impact of biomass burning in equatorial Africa on the downward surface shortwave irradiance: Observations versus calculations. *J. Geophys. Res.*, **101**, 22 833–22 844.
- Kotchenruther, R., and P. V. Hobbs, 1998: Humidification factors of aerosols from biomass burning in Brazil. *J. Geophys. Res.*, **103**, 32 081–32 090.
- Lenoble, J., 1991: The particulate matter from biomass burning: A tutorial and critical review of its radiative impact. *Global Biomass Burning, Atmospheric, Climate, and Biospheric Implications*. J. S. Levine, Ed., MIT Press, 381–386.
- Li, Z., 1995: Intercomparison between two satellite-based products of net surface shortwave radiation. *J. Geophys. Res.*, **100**, 3221–3232.
- , 1998: Influence of absorbing aerosols on the inference of solar surface radiation budget and cloud absorption. *J. Climate*, **11**, 5–17.
- Liou, K. N., Q. Fu, and T. P. Ackerman, 1988: A simple formulation of the delta-four-stream approximation for radiative transfer parameterizations. *J. Atmos. Sci.*, **45**, 1940–1947.
- Martins, J. V., P. V. Hobbs, R. E. Weiss, and P. Artaxo, 1998: Sphericity and morphology of smoke particles from biomass burning in Brazil. *J. Geophys. Res.*, **103**, 32 051–32 058.
- McClatchey, R. A., R. W. Fenn, J. E. A. Selby, F. E. Volz, and J. S. Garing, 1972: Optical properties of the atmosphere. Air Force Cambridge Research Lab. Rep. AFCRL-72-0497, Bedford, MA.
- Penner, J. E., R. E. Dickinson, and C. A. O'Neill, 1992: Effects of aerosol from biomass burning on the global radiation budget. *Science*, **256**, 1432–1434.
- Pinker, R. T., and I. Laszlo, 1992a: Global distribution of photosynthetically active radiation as observed from satellites. *J. Climate*, **5**, 56–65.
- , and —, 1992b: Modeling surface solar irradiance for satellite applications on a global scale. *J. Appl. Meteor.*, **31**, 194–211.
- Prins, E. M., J. M. Feltz, W. P. Menzel, and D. E. Ward, 1998: An overview of GOES-8 diurnal fire and smoke results for SCAR-B and the 1995 fire season in South America. *J. Geophys. Res.*, **103**, 31 821–31 836.
- Reid, J. S., P. V. Hobbs, C. Liou, J. V. Martins, R. E. Weiss, and T. F. Eck, 1998a: Comparisons of techniques for measuring shortwave absorption and black carbon content of aerosols from biomass burning in Brazil. *J. Geophys. Res.*, **103**, 32 031–32 040.
- , —, R. J. Ferek, D. R. Blake, J. V. Martins, M. R. Dunlap, and C. Liou, 1998b: Physical, chemical and optical properties of regional hazes dominated by smoke in Brazil. *J. Geophys. Res.*, **103**, 32 059–32 080.
- Robock, A., 1988: Enhancement of surface cooling due to forest fire smoke. *Science*, **242**, 911–913.
- Ross, J. L., P. V. Hobbs, and B. N. Holben, 1998: Radiative characteristics of regional hazes dominated by smoke from biomass burning in Brazil: Closure tests and direct radiative forcing. *J. Geophys. Res.*, **103**, 31 925–31 942.
- Schiffer, R. A., and W. B. Rossow, 1983: The International Satellite Cloud Climatology Project (ISCCP): The first project of the World Climate Research Program. *Bull. Amer. Meteor. Soc.*, **64**, 779–784.
- Setzer, A. W., and M. C. Perreira, 1991: Amazonia biomass burnings in 1987: An estimate of their tropospheric emissions. *Ambio*, **20**, 19–22.
- Waliser, D. E., W. D. Collins, and S. P. Anderson, 1996: An estimate of the surface shortwave cloud forcing over the western Pacific during TOGA COARE. *Geophys. Res. Lett.*, **23**, 519–522.
- Westphal, D. L., and O. B. Toon, 1991: Simulations of microphysical, radiative, and dynamical processes in a continental-scale forest fire smoke plume. *J. Geophys. Res.*, **96**, 22 379–22 400.
- Whitlock, C. H., and Coauthors, 1995: First global WCRP shortwave surface radiation budget data set. *Bull. Amer. Meteor. Soc.*, **76**, 905–922.